

## Force dynamics in weakly vibrated granular packings

Paul Umbanhowar<sup>1</sup> and Martin van Hecke<sup>2</sup>

<sup>1</sup>*Department of Physics and Astronomy, Northwestern University, Evanston, Illinois 60208, USA*

<sup>2</sup>*Kamerlingh Onnes Lab, Leiden University, P.O. Box 9504, 2300 RA Leiden, The Netherlands*

(Received 6 October 2004; published 19 September 2005)

Variations in the oscillatory force  $\tilde{F}_b$  on the bottom of a rigid, grain filled column, reveal rich granular dynamics when the column is vertically vibrated with an acceleration amplitude significantly *less* than the gravitational acceleration at the earth's surface. Large changes in  $\tilde{F}_b$  occur even though the maximum relative motion of the container bottom with respect to the wall is less than 2 nm. For previously unshaken packings or high frequencies,  $\tilde{F}_b$ 's dynamics are dominated by grain motion. For moderate driving conditions in already shaken samples, grain motion is virtually absent, but  $\tilde{F}_b$  nevertheless exhibits strongly nonlinear and hysteretic behavior, evidencing a granular regime dominated by nontrivial force-network dynamics.

DOI: 10.1103/PhysRevE.72.030301

PACS number(s): 45.70.-n, 05.45.-a, 43.25.+y

Granular media consist of macroscopic solid grains which interact via dissipative, repulsive contact forces. Thermal energy is inconsequential, and granulates *jam* in random configurations unless sufficient mechanical energy is supplied, for example by shearing or shaking [1]. For sinusoidally, vertically vibrated granular media the driving strength is characterized by the nondimensional acceleration amplitude,  $\Gamma = A(2\pi f)^2/g$ , where  $A$  is the displacement amplitude,  $f$  is the oscillation frequency, and  $g$  is the gravitational acceleration at the Earth's surface. In the well-studied case of  $\Gamma \geq 1$ , grains periodically lose contact with and subsequently impact the oscillating container. Collisions, as well as the accompanying relative motion between grains and wall, inject energy into the system that drives grain rearrangements producing, for example, compaction, convection, segregation, and standing waves [2,3].

In contrast, the  $\Gamma < 1$  regime has not received nearly as much attention. Does grain motion still occur here, and if so, under what circumstances? In the absence of grain motion, is the injected energy sufficient to excite variations of the force network? We address these questions by examining the oscillatory force on the container bottom,  $\tilde{F}_b$ , in a weakly vibrated, rigid column filled with granular material of mass  $M$  [Fig. 1(a)]. Even though we use  $\Gamma < 1$  and an extremely stiff container/force transducer, the grain system continues to exhibit rich dynamics as evidenced by large changes in  $\tilde{F}_b$ .

We will identify compaction of loose samples and high frequency driving as cases where the dynamics is dominated by grain rearrangements. With moderate, low frequency driving in previously shaken samples, however, relative grain motion is minute but variations in the force configuration remain substantial. Weak vibrations thus excite strongly nonlinear and glassy dynamics of the force network. Large force variations in the absence of grain rearrangement are possible because the grain and deformation scales are separated by many orders of magnitude [4]: a 700  $\mu\text{m}$  diameter bronze sphere is compressed only  $\sim 100$  nm under the terrestrial weight of 1000 additional identical spheres [5]. The implication of this finding is broad: the physical properties of apparently quiescent granular media are not fixed, and even subtle variations in the character and duration of perturbations can be significant.

*Experimental setup:* Nearly-spherical bronze particles sieved between 0.61 and 0.70 mm are poured into a smooth cylindrical tube with a detached bottom which is supported by a rigid piezoelectric force sensor (stiffness 2.5 GN/m). The *entire assembly* is vertically oscillated with a small sinusoidal displacement [Fig. 1(a)]. An accelerometer attached to the tube measures the time-resolved acceleration  $\gamma(t)$  which, for most driving conditions, is harmonic, equaling  $\Gamma \sin(2\pi ft)$ . The measured force is sensitive to temperature drift. The entire assembly is therefore placed in a temperature controlled enclosure maintained slightly above room temperature (temperature fluctuations  $\pm 10$  mK, humidity 5%–10%); grains are equilibrated in the enclosure prior to use.

The deflection of the relatively compliant force sensors used in most previous studies is large compared to the defor-

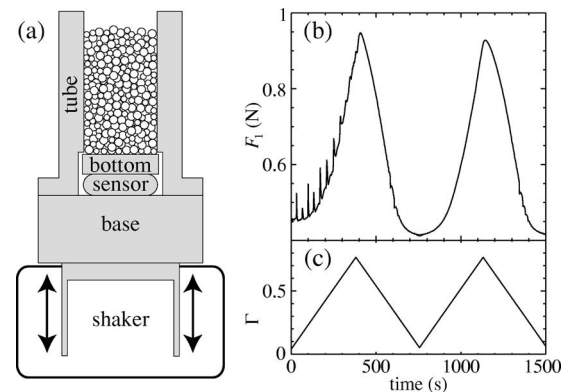


FIG. 1. (a) Schematic of the experiment showing the piezo force sensor mounted between the “bottom” and the “base” (diameter  $\times$  height:  $32 \times 12$  mm and  $89 \times 62$  mm, respectively), with a cylindrical tube (inner/outer diameter 30/55 mm, height 113 mm) which is attached only to the base. The small  $\sim 100$   $\mu\text{m}$  gap between the tube and bottom plate prevents grains from becoming trapped. Shaded parts are rigidly connected and move in unison. The sensor signal is used to obtain  $\tilde{F}_b$ , the amplitude of the oscillatory component of the vertical force exerted on the bottom plate by the grains. (b,c) Nonlinear response of a column filled with 200 g of 0.61–0.70 mm diameter bronze particles under sweeps of the vibration amplitude  $\Gamma$  for  $f=80$  Hz;  $F_1$  denotes the calibrated ratio of the first harmonic of  $\tilde{F}_b$  to  $\Gamma$  [see Eq. (1)].

mation of hard grains like steel or glass; the granular force configuration is then completely altered due to relative motion between force probe and grains/walls. In contrast, our tube/sensor assembly is effectively a *solid* container since the maximal deflection of the piezo is less than 2 nm, which ensures that the measured force variations are intrinsic to the granular medium [6–8].

In our experiment, the force sensor measures the total *oscillatory force*,  $\tilde{F}$ , which is the sum of the inertial force generated by the acceleration of the bottom plate and sensor, with effective mass  $M_0$ , and the oscillatory bottom force  $\tilde{F}_b$  resulting from the acceleration of material in the column (which can have harmonics),

$$\tilde{F} = \Gamma M_0 g \sin(2\pi ft) + \Gamma \sum_{n=1}^{\infty} F_n \sin(2\pi nft - \phi_n). \quad (1)$$

To calibrate the signal,  $\tilde{F}$  was measured for a range of  $f$  and  $\Gamma$ , both with and without solid test masses attached to the bottom plate. The value of  $\tilde{F}$  for the empty system allows us to subtract the term proportional to  $\Gamma M_0 g$ , after which  $F_1$  is found to be proportional to the test mass and independent of  $\Gamma$  (the definition of  $F_n$  isolates the trivial scaling with  $\Gamma$ ). The higher harmonics  $F_2, F_3, \dots$  are negligible in this case.

It will be important to distinguish a *contact regime* where grains do not slide with respect to the column, and a *sliding regime* where they do. In the contact regime,

$$Mg\Gamma \sin(2\pi ft) = \tilde{F}_w + \tilde{F}_b, \quad (2)$$

where  $\tilde{F}_w$  is the oscillatory vertical component of the frictional wall-force. However, Eq. (2) is violated in the sliding regime. For various experimental situations, we have checked whether Eq. (2) applies by placing a grain filled container with a closed bottom directly on the bottom plate [9]. For this arrangement, the sensor measures the sum  $\tilde{F}_w + \tilde{F}_b$ ; when the sensor signal remains purely harmonic, the system is in the contact regime, when (strong) nonlinearities exist, it is in the sliding regime.

*Basic phenomenology:* When a column of grains rests on the force sensor,  $F_1$  displays strongly nonlinear and hysteretic behavior of the granulate [see Figs. 1(b) and 1(c)]. The most apparent feature is the strong and nonlinear dependence of  $F_1$  on  $\Gamma$  [e.g.,  $F_1(\Gamma=0.5) \approx 2F_1(\Gamma=0.05)$ ], even for low driving frequencies. ( $F_1$  is independent of  $\Gamma$  for a solid mass placed on the bottom.) The spikes in  $F_1$  during the initial ramp are another general feature, and are caused, as we will show, by compaction of the material. The asymmetry of  $F_1(\Gamma)$  indicates hysteresis and memory effects. We stress that the strength of these features does not vary significantly for driving frequencies from 16 to 300 Hz. The phenomena evident in Fig. 1(b) are essentially quasistatic and are not associated with the excitation of sound waves (see below). These features are caused by a mixture of contact and sliding dynamics. Although our main interest is in the contact regime, we first discuss two examples of grain-sliding dominated phenomena: *spiking* and *impact*.

*Spiking:* “Spikes,” such as those shown in Fig. 1(b), occur

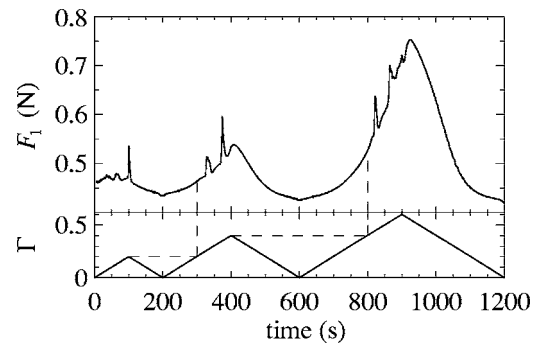


FIG. 2. Spikes observed for  $f=80$  Hz and  $M=200$  g in a previously unshaken packing. Sweeps of increasing magnitude in  $\Gamma$  illustrate that spikes only occur when  $\Gamma$  exceeds its previous maximum value.

when  $\Gamma$  is ramped up in loosely packed samples, which are formed by placing the end of a funnel on the bottom of the container, filling the funnel with material, and then slowly retracting the funnel. Figure 2 illustrates that spikes only occur in “fresh” territory, i.e., when  $\Gamma$  is increased beyond its previous maximum value. The specific  $\Gamma$  values where spikes occur vary from run to run, and hence are not resonant effects. There is no substantial frequency dependence: qualitatively similar spikes occur for  $16 \leq f \leq 300$  Hz, and even switching to a different frequency while ramping  $\Gamma$  does not appreciably alter the range where spiking occurs. After  $\Gamma$  has been swept up to a value near one, reduced, and then maintained below this maximum value, spikes are not observed, and we refer to such samples as *nonspiking*.

During a spike, which typically lasts for 1000’s of oscillation cycles,  $\phi_1$  shifts significantly (indicating dissipation) and  $\tilde{F}_b$  is strongly nonsinusoidal. Appreciable deviations from harmonic behavior also occur in a closed bottom container placed directly on the sensor—indicating that during a spike, material slides. Spikes are associated with compaction: the free surface is lower after a spike has occurred, and gently poured columns with lower initial density produce more spikes than less gently poured ones with higher initial density. Underlying these phenomena is presumably that the frictional forces at the wall in granular columns are fully mobilized [6,10]. Therefore even weak vibrations may cause slipping and compaction and stronger vibrations may then cause further slipping and compaction.

*Impact vs contact:* For nonspiking samples we distinguish between the contact regime where Eq. (2) is satisfied, and a sliding regime referred to as “impact” where Eq. (2) is violated. Figure 3(a) illustrates that for low frequencies  $F_1$  increases smoothly with  $\Gamma$ , while for higher frequencies there is a sudden upturn and peak in  $F_1$ . In the vicinity of and above this transition, both  $\gamma(t)$  and  $\tilde{F}_b$  are strongly anharmonic—as when grains periodically slide and then impact the bottom for  $\Gamma > 1$ .  $\tilde{F}_b$  becomes strongly anharmonic for the closed bottom container as well. Below this transition,  $\gamma(t)$  for both containers and  $\tilde{F}_b$  for the closed bottom container remain sinusoidal; this is the contact regime. The physics underlying the force dynamics in the contact regime is thus a smooth, periodic transfer of grain weight between

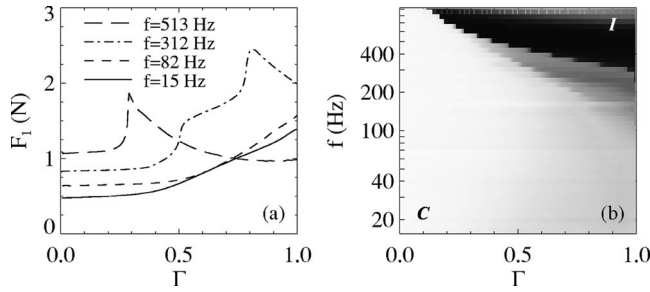


FIG. 3. Contact and impact regimes ( $M=200$  g): (a)  $F_1(\Gamma, f)$  is smooth at low frequencies, but increases abruptly and peaks for higher frequencies (data is vertically offset for clarity). (b) Grey-scale intensity plot of nonlinearity  $\mathcal{N}(\Gamma, f) \equiv F_1(\Gamma, f) - F_1(0, f)$  (white,  $\mathcal{N}=0$ ; black,  $\mathcal{N}=1$ ) indicating the contact (C) and impact (I) regimes.

wall and bottom, while in the impact regime, grains slide substantially and periodically impact the sensor.

Figure 3(b) displays the strength of the nonlinearity of  $F_1$  as function of  $\Gamma$  and  $f$ —the rapid increase in nonlinearity marks the onset of impact. For high frequencies ( $f \approx 1$  kHz), the impact regime occurs for surprisingly small  $\Gamma$  ( $\approx 0.1$ ). Here the higher harmonics  $F_2, F_3, \dots$  become very strong and  $F_1$  actually diminishes [see Fig. 3(b) for  $f > 800$  Hz].

Apparently, impact for  $\Gamma < 1$  is due to the excitation of resonant granular sound waves. Typical sound speeds are of the order of  $100 \text{ ms}^{-1}$  [11], so in our 10 cm deep column we expect a resonant response around 1 kHz. This picture is consistent with findings of Yanagida *et al.* [9] in studies of the resonant response of grain filled closed bottom containers for small  $\Gamma$ , and it is also consistent with the shift of the impact transition to higher frequencies for smaller  $M$  (this also excludes a trivial resonance of the apparatus). The  $\Gamma$  dependence of this transition is not fully understood.

*Contact regime nonlinearity:* We now explore the nonlinear response of nonspiking samples in the contact regime as a function of  $M$  and  $\Gamma$ . The frequency is fixed at 80 Hz, since in the contact regime the grain response varies only weakly with  $f$ .

Figure 4(a) illustrates that the small mass behavior is independent of  $\Gamma$ , and that the grains are supported entirely by

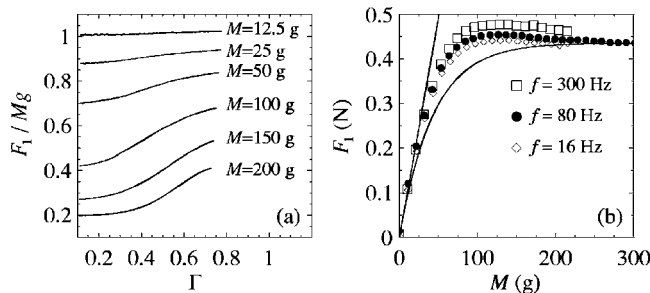


FIG. 4. Nonlinearity of  $F_1$  with  $\Gamma$  and total grain mass  $M$ . (a)  $F_1(\Gamma)/Mg$  for various filling fractions ( $f=80$  Hz). For larger  $M$  and fixed  $\Gamma$ , the weight fraction on the bottom decreases. (b)  $F_1$  as function of  $M$  in the linear regime ( $\Gamma=0.05$ ) for  $f=16, 80,$  and  $300$  Hz, compared to a linear response (straight line) and a Janssen-type response  $F_1/F_{\text{sat}} = 1 - \exp(-Mg/F_{\text{sat}})$  for  $F_{\text{sat}}=0.435$  N.

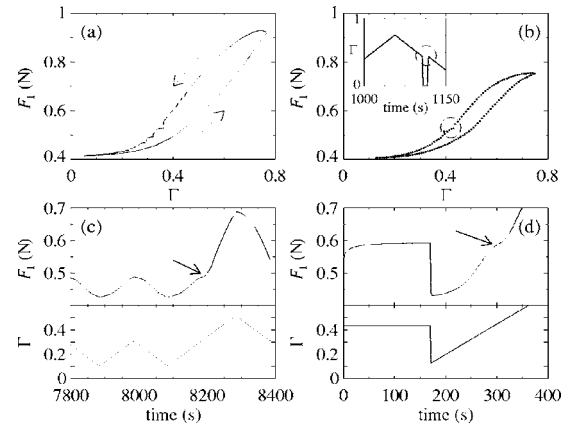


FIG. 5. Memory effects ( $M=200$  g and  $f=80$  Hz). (a) Hysteresis loop. (b) Hysteresis persists when  $\Gamma$  is suddenly set to zero and then rapidly ramped back up, indicated by the circle (see inset for details of ramp). (c, d) Two examples of subtle memory effects.

the bottom since  $F_1 \approx Mg$ . For larger masses and correspondingly higher fill heights, wall forces start to play a role since  $F_1 < Mg$  and the material's response becomes increasingly nonlinear with  $\Gamma$ .

For small  $\Gamma$  the response is linear in  $\Gamma$ : for  $\Gamma \approx 0.05$ ,  $\bar{F}_b$  is harmonic ( $< 1\%$  distortion) and in-phase with the acceleration, and  $F_1$  varies less than  $1\%$  for  $0 < \Gamma < 0.1$ . We study  $F_1(M)$  as a function of increasing mass  $M$  at  $\Gamma \approx 0.05$  by incrementally pouring grains from a height of approximately 10 cm above the grain surface. Figure 4(b) illustrates that  $F_1$  grows proportionally with  $M$  for small masses, but then rapidly saturates to  $F_1^{\text{sat}} \approx 0.435$  N.  $F_1(M)$  is only weakly frequency dependent, again indicating that in the contact regime a well-defined quasistatic regime is probed. Note that for all  $f$  a small overshoot occurs for intermediate values of  $M \approx 100$  g.

This behavior is reminiscent of the Janssen effect for which the steady bottom force  $\bar{F}_b$  goes as [6,10,12]:

$$\bar{F}_b = \bar{F}_{\text{sat}}[1 - \exp(-Mg/\bar{F}_{\text{sat}})], \quad (3)$$

where  $\bar{F}_{\text{sat}}$  is the saturation force. Figure 4(b) shows, however, that the amplitude of the first harmonic of the oscillatory bottom force  $F_1$  significantly deviates from the static Janssen result. We conclude that, even in the limit of weak vibrations, the oscillatory force  $\bar{F}_b$  is *not* simply related to the steady force  $\bar{F}_b$ .

*Hysteresis and memory:* When  $\Gamma$  is ramped up and down in the nonlinear regime, Fig. 5(a) indicates that  $\bar{F}_b$  is hysteretic. The magnitude of hysteresis is only weakly dependent on the driving frequency and increases with  $M$  and  $\Gamma$  similar to the magnitude of overall nonlinearity. The hysteresis is nearly independent of the sweep speed (for sweep durations longer than  $\approx 100/f$ ), and the force configuration thus depends on the driving history. Similar hysteretic behavior, known as the Branly effect, has been observed in the electrical resistance of metal bead packs when the current is ramped up and down [13]. Figure 5(b) illustrates that these configurations can be retained, since the system returns to

the upper branch of the hysteresis loop after the driving is switched off and then rapidly ramped up again. The system exhibits additional subtle memory effects: after a fully annealed system is subject to a number of small amplitude sweeps in  $\Gamma$ , and then  $\Gamma$  is ramped beyond the peak value of the small sweeps, a clear kink in the  $F_1$  curve is exhibited [Figs. 5(c) and 5(d)]. When a fully annealed system is driven at a fixed  $\Gamma$ , it “remembers” this value when  $\Gamma$  is rapidly decreased and then ramped past the initial fixed value [Figs. 5(e) and 5(f)].

*Discussion:* Our experiments exhibit rich dynamical behavior of weakly excited ( $\Gamma < 1$ ) granular media which can be dominated by either grain motion or by contact force variations. That grain motion and compaction occur in previously unshaken samples vibrated at low frequencies and for  $\Gamma < 1$  is maybe not surprising, although we are unaware of systematic studies of compaction in this regime [3,14] The most striking phenomena are the nonlinearities, memory effects, and hysteresis of the force which occur for weakly driven, preshaken samples in the absence of appreciable grain motion. We have not identified any theoretical or numerical descriptions of these surprisingly strong effects. Ex-

ploratory experiments in various columns with rough walls and for particles of different sizes produce qualitatively similar results and further illustrate the robustness of these phenomena.

How should weakly vibrated granular systems be viewed? A weakly driven granular assembly apparently amplifies the local nonlinearities present in the contacts between grains [5,15]. We propose that force networks “activated” by weak vibrations explore many different configurations consistent with the overall boundary conditions for the stress [4,16]. Such activated force networks could possibly play a role in creep flows, which occur far away from shear zones, and more generally in any granular system in which tiny relative grain motions are excited. In this sense, weakly driven granulates cannot be thought of as ordinary solids, and they are definitely not static or even quasi-static when many physical properties other than relative grain position are of interest.

The authors thank CATS and the Netherlands Organization for Scientific Research (NWO) who supported visits to NWU during which this work was carried out.

- 
- [1] A. J. Liu and S. R. Nagel, *Nature (London)* **396**, 21 (1998); C. S. O’Hern *et al.*, *Phys. Rev. Lett.* **88**, 075507 (2002).
  - [2] G. H. Ristow, *Pattern Formation in Granular Materials* (Springer-Verlag, Berlin, 2000).
  - [3] P. Richard M. Nicodemi, R. Delannay, P. Ribière, and D. Bideau, *Nat. Mater.* **4**, 121 (2005).
  - [4] J. H. Snoeijer *et al.*, *Phys. Rev. Lett.* **92**, 054302 (2004).
  - [5] K. L. Johnson, *Contact Mechanics* (Cambridge University Press, Cambridge, 1987).
  - [6] G. Ovarlez, C. Fond, and E. Clément, *Phys. Rev. E* **67**, 060302(R) (2003).
  - [7] L. Vanel *et al.*, *Phys. Rev. E* **60**, R5040 (1999).
  - [8] G. D’Anna and G. Gremaud, *Nature (London)* **413**, 407 (2001); G. D’Anna *et al.*, *Europhys. Lett.* **61**, 60 (2003).
  - [9] T. Yanagida A. J. Matchett, J. M. Coulthard, B. N. Asmar, P. A. Langston, and J. K. Walters, *AIChE J.* **48**, 2510 (2002); A. J. Matchett and T. Yanagida, *Powder Technol.* **137**, 148 (2003).
  - [10] H. A. Janssen, *Z. Ver. Dt. Ing.* **39**, 1045 (1895).
  - [11] J. D. Goddard, *Proc. - R. Soc. Edinburgh, Sect. A: Math.* **430**, 105 (1990); C. H. Liu and S. R. Nagel, *Phys. Rev. Lett.* **68**, 2301 (1992).
  - [12] P. G. de Gennes, *Rev. Mod. Phys.* **71**, 374 (1999).
  - [13] S. Dorbolo, M. Ausloos, and N. Vandewalle, *Phys. Rev. E* **67**, 040302(R) (2003).
  - [14] H. Bontebal, J. Dijksman, and M. van Hecke (unpublished).
  - [15] F. Alonso-Marroquin and H. J. Herrmann, *Phys. Rev. Lett.* **92**, 054301 (2004).
  - [16] J. P. Bouchaud, in *Proceedings of the 2002 Les Houches Summer School on Slow Relaxations and Nonequilibrium Dynamics in Condensed Matter*.